91602
new 82-10

COMPLIMENTARY COPY
Please Credit Ontario Hydro Research if
Reproduced in Whole or in Part

LEGAL NOTICE

This report was prepared by Ontario Hydro and, while effort has been made to assure the accuracy and applicability of the material contained herein, neither Ontario Hydro nor any person acting on its behalf:

(a) makes any warranty, express or implied with respect to the use of any information, apparatus, method or process disclosed in this report or that such use may not infringe privately owned rights; or

(b) assumes any liabilities with respect to the use of, or for damages resulting from the use of, any information, apparatus, method or process disclosed in this report.

ontario hydro
research division

THE HIGH CYCLE FATIGUE BEHAVIOUR OF DARLINGTON UNIT 2 GENERATOR ROTOR MATERIAL

Report No. 91-44-K

W.K. Lee - Engineer
D.W. Carpenter - Technologist
Fracture Technology Section
Metallurgical Research Department

ABSTRACT

A test program was undertaken by Ontario Hydro Research and Engineering Material Research to determine the high cycle fatigue behaviour at 100°C of material from a failed Darlington Unit 2 generator rotor shaft. Prediction methods, including the extensively used Normal Distribution and the Arc Sine Function proposed by the shaft's manufacturer, were used to estimate the fatigue endurance limit. The experimental results, supported by an overview of current practices, suggest that we can predict with confidence the fatigue endurance limit corresponding to 50% probability of failure. An appropriate safety factor should then be applied to this value during the design stage.

job	file	date	report no.
84-118-452	826.233	April 12, 1991	91-44-K

91602
new 82-10

ontario hydro
research division

EXECUTIVE SUMMARY

THE HIGH CYCLE FATIGUE BEHAVIOUR OF DARLINGTON UNIT 2 GENERATOR ROTOR MATERIAL

W.K. Lee and D.W. Carpenter
Fracture Technology Section
Metallurgical Research Department

OBJECTIVE: To determine the high cycle fatigue behaviour of material from a failed Darlington Unit 2 Generator Rotor.

EXPERIMENTS: Parallel test systems were set up at the Research Division (OHRD) and an external company, Engineering Material Research (EMR) to carry out high cycle fatigue tests at 100°C. The loading system and procedures conformed to ASTM standards.

RESULTS:

1. There are no significant differences between these test results and those obtained by ASEA BROWN BOVERI. A wider data scatter in the N6, R=-1 and N9, R=0 test conditions was observed in the OHRD and EMR test results, although the same test procedures were used. All results showed good correlation between the applied cyclic stress and the probability of failure using either the Normal Distribution or the Arc Sine Distribution.

2. The failure strength corresponding to 50% probability of failure (median fatigue strength) from the two distributions was close. Projected "lower bound" failure strengths varied more significantly with the distribution used.

3. In view of the frequent use of the Normal Distribution and the uncertainties associated with prediction from limited data, we recommend that the median fatigue strength together with an appropriate safety factor should be used by the designers. The lower bound estimates can be used as a guide for selecting the safety factor.

B.M
B.M

job	file	date	report no.
85-118-452	826.233	April 12, 1991	91-44-K

TABLE OF CONTENTS

		PAGE
1.0	INTRODUCTION	1
2.0	THE EXPERIMENTS	1
3.0	RESULTS	2
4.0	DATA ANALYSIS	3
4.1	The Percentage of Failures	3
4.2	Interpretation of Fatigue Data Using the Normal Distribution	3
4.3	Interpretation of Fatigue Data Using the Arc Sine Distribution	3
4.4	Analysis of All Data (OH (OHRD & EMR), ABB)	4
4.5	Haigh Diagram	6
5.0	DISCUSSION	6
5.1	Current Understanding of the Fatigue Limit	6
5.2	Comparison Between the Normal Distribution & the Arc Sine Method	7
6.0	SUMMARY	8
ACKNOWLEDGEMENT		8
REFERENCES		9
APPENDIX I - Results of Strain Gauge Measurements to Determine the Axial Alignment		19
APPENDIX II - Experimental Results		23
APPENDIX III - The Percent of Failures		29
DISTRIBUTION		last pge

ontario hydro
research division

TO: M.A. Machacek
Manager of Engineering
Darlington Project

THE HIGH CYCLE FATIGUE BEHAVIOUR OF DARLINGTON UNIT 2 GENERATOR ROTOR MATERIAL

1.0 INTRODUCTION

During the commissioning of Darlington Unit 2, excessive vibration in the generator rotor led to the discovery of a fretting initiated crack in the body of the rotor. Details of the failure analysis have been reported elsewhere/1/. Since the rotor material is a modified version of the manufacturer ASEA BROWN BOVERI (ABB)'s standard material (St 577), there were concerns about the material's resistance to fatigue damage and the lack of material data. The material data are required for the formulation of an interim solution for the other Darlington units and the design of the long term replacement rotor.

The test program reported here addresses the high cycle fatigue strength of the St OH 700 material used for the generator rotor. The following sections present the results of laboratory tests carried out at Ontario Hydro Research Division (OHRD) and at an outside company, Engineering Material Research (EMR). The data generated by ABB was also examined. All three laboratories obtained very similar results and a fatigue strength was derived for design application in which an appropriate safety factor is required.

2.0 THE EXPERIMENTS

The high cycle fatigue tests on the failed rotor material were carried out at 100°C on servo-hydraulic frames designed for axial push-pull loading. Hour-glass fatigue specimens, with the dimensions shown in Figure 1, were machined from the Unit 2 rotor close to the failure site. Figure 2 shows the locations of all the specimens which have the cyclic loads applied parallel to the longitudinal axis of the rotor. Two specimens in series, along the longitudinal direction, were prepared from each location. Chemical compositions and mechanical properties of the St OH 700 rotor material are shown in Table I and Table II.

In general, the test procedures followed the recommended guidelines in the ASTM standards/2,3/. The schematic diagram for the set-up is shown in Figure 3. Two similar sets of loading fixtures were prepared, one at OHRD and the other at EMR. The alignment of the loading train was checked through strain measurements and found to be within the ASTM specifications, the results are in Appendix I.

All fatigue tests were conducted using load control and a sinusoidal waveform. The test matrix included the following parameters: two R-ratios (minimum load/maximum load) of -1 and 0 , and two types of surface finish (N6 and N9). N6 has a surface roughness of 0.8 μm and N9 has a surface roughness of 6.3 μm. The failure criterion was the complete fracture of the test specimen. The test specimen was called a run-out when the total number of fatigue cycles reached 10 million. The run-outs were assumed to have an infinite fatigue life.

TABLE I
CHEMICAL COMPOSITIONS IN Wt%/1/

ELEMENT	LOCATION RIM	MID RADIUS	BORE	SPECIFIED VALUES (ST 577)
Carbon	0.25	0.24	0.23	0.22-0.32
Manganese	0.26	0.25	0.26	0.2-0.5
Silicon	0.019	0.018	0.018	0.3 max.
Nickel	3.44	3.72	3.68	3.2-4.0
Chromium	1.53	1.57	1.47	1.2-1.8
Molybdenum	0.38	0.37	0.37	0.3-0.6
Vanadium	0.093	0.093	0.089	0.05-0.15
Phosphorus	<0.005	0.005	<0.005	0.015 max.
Sulphur	0.005	0.005	0.005	0.018 max.
Tin	0.01	0.01	0.01	NS
Antimony	0.015	0.015	0.015	NS
Arsenic	<0.02	<0.02	<0.02	NS
Copper	0.1	0.1	0.1	NS
Aluminum	0.01	0.012	0.013	NS

NS = Not Specified

TABLE II
ROOM TEMPERATURE TENSILE PROPERTIES/1/

ORIENTATION & LOCATION	UTS (MPa)	YS (MPa)	% ELONGATION	% REDUCTION OF AREA
Axial Rim	888	787	25.5	71
Axial Bore	860	764	28.0	61
Tangential Rim	893	794	22.5	60.5
Tangential Bore	855	751	24.5	68
ABB Specs. Rim	800-950	700	18/16/14	NS
Bore	NS	650	14	NS

NS = Not Specified

3.0 RESULTS

Table I in Appendix II lists all the experimental data generated at OHRD and EMR. If the failures were outside the minimum gauge diameter or at a position where the thermocouple was attached, the data were excluded in the analysis. Some specimens were tested at relatively high peak stresses since they were used initially to estimate the range of test loads. In general, repeat tests

were performed for each stress/R-ratio combination.

Figures 4 & 5 show the S-N data at 100 C, including the results (listed in Table II-II in Appendix II) produced by ABB; the number of fatigue cycles (N) is plotted against the cyclic stress amplitude (S) which is one half of the difference between the maximum and the minimum applied stress. The data labelled 'OH' include the EMR results.

4.0 *DATA ANALYSIS*

Since it is not economically feasible to test for very long periods of time such that all test specimens will be run-outs, multiple tests at higher stress amplitudes were carried out in order to estimate the stress amplitude (hereafter called fatigue strength) corresponding to a particular fraction of failure. Several schemes for fatigue strength prediction are available, the following sections outline methods and demonstrate applications to the data.

4.1 *The Percentage of Failures*

All prediction methods require an estimate of the percent of failure for the population from the limited experimental data. This estimated value is always different from the true population value because of the small sample size and can lead to deviation in the predicted fatigue strength. Furthermore, experimental uncertainties associated with the loading system may also contribute to data scatter. The estimate is taken to be the probability of failure and is assumed to be a distributed function of the fatigue strength. In this analysis, we have only considered the Normal Distribution and the Arc Sine Distribution. The procedures used to calculate the percent of failures for the population and the results are shown in Appendix III.

4.2 *Interpretation of fatigue data using the Normal Distribution*

The Normal Distribution method to determine the fatigue strength was well documented by R.E. Little/7/. The percent of failure is first converted to standard deviation units based on the Normal Distribution, the final result is a linear plot of the fatigue strength versus the standard deviation values. The percentage of failure at each stress level is expressed as a probability value (between 0 and 1). Assuming a Normal Distribution for the fatigue strength, the median strength value will be at the 50% failure point (or 0.5 probability). As shown in Figure 6, the probability of failure values on the y axis can be correlated with the number of standard deviations on the x axis; the 0.5 probability corresponds to the 0.0 median value on the x axis. A plot of the experimental cyclic stress amplitude versus the standard deviation values (obtained from Figure 6) will give us the median fatigue strength corresponding to the 0.0 standard deviation location.

As an example, for the set of specimens with N6 surface finish and a loading ratio of 0, the above method produced a straight line fit with a correlation coefficient of 0.95. Figure 7 is the plot of the fatigue strength versus the standard deviation, using the i/(n+1) formula (eqn. A(1) in Appendix III).

4.3 *Interpretation of Fatigue Data using the Arc Sine Distribution*

ABB's data as well as our own laboratory data were analyzed using the Arc Sine method/6/. The experimental cyclic stress amplitudes were correlated with the percentages of failures (as defined in section 4.1) using the following equation.

$$\sigma = A + B \{ \arcsin (\sqrt{p'}) \} \quad (1)$$

where
- σ – stress amplitude
- A – intercept, fatigue strength at zero percent of failure
- B – slope of straight line fit
- p' – percent of failure/100, equivalent to probability of failure
- arc sin – function expressed in radian

The fatigue strength at zero probability of failure is the value of A obtained through straight line least-squares fit of equation (1) using the experimental data set. In Normal Distribution, there is no zero probability of failure.

4.4 ***Analysis of All Data (OH (OHRD & EMR),ABB)***

The Normal distribution and the Arc Sine distribution were applied to all the 100 C test data. For each set of test conditions, the data were least-squares fitted to a straight line equation using the methods outlined in sections 4.2 and 4.3. The fatigue strength corresponding to the desired probability of failure (P) was then calculated from the least-squares equation.

The results are in Table IIIa for the normal distribution using eqn. A(1), Table IIIb for the normal distribution using eqn. A(2), Table IIIc for the arc sine distribution using eqn. A(4). The column $P_{0.01}$ represents the fatigue strenth at 0.01 probability of failure; $P_{0.5}$ is the fatigue strength with a 0.5 probability of failure; r is the correlation coefficient for the least-squares fit.

The lowest $P_{0.01}$ fatigue strength values from Table IIIa and the zero probability of failure strengths from the Arc Sine function were marked on Fig. 4 & 5.

TABLE IIIa

Normal Distribution Using i/(n+1), Eqn. A(1)

	ABB			OH			COMBINED		
TEST CONDI-TIONS	P 0.01	P 0.5	r	P 0.01	P 0.5	r	P 0.01	P 0.5	r
N6,R=-1	387	450	0.9	408	460	0.8	398	457	0.8
N6,R=0	302	351	0.97	312	360	0.99	302	355	0.95
N9,R=-1	269	313	0.98	253	331	0.97	263	320	0.84
N9,R=0	244	284	0.99	218	271	0.65	225	278	0.7

TABLE IIIB

Normal Distribution Using (i-3/8)/(n+1/4), Eqn. A(2)

	ABB			OH			COMBINED		
TEST CONDI-TIONS	P 0.01	P 0.5	r	P 0.01	P 0.5	r	P 0.01	P 0.5	r
N6,R=-1	400	451	0.92	418	459	0.84	410	457	0.85
N6,R=0	311	351	0.97	321	359	0.99	312	355	0.95
N9,R=-1	275	312	0.98	267	331	0.98	272	319	0.84
N9,R=0	251	283	0.99	226	271	0.65	234	278	0.73

TABLE IIIC

Arc Sine Distribution, Eqn. A(4)

	ABB			OH			COMBINED		
TEST CONDI-TIONS	P 0	P 0.5	r	P 0	P 0.5	r	P 0	P 0.5	r
N6,R=-1	410	450	0.95	435	452	0.83	428	452	0.82
N6,R=0	316	350	0.99	326	359	0.99	320	354	0.96
N9,R=-1	276	310	0.98	278	326	0.99	286	316	0.85
N9,R=0	248	280	1.0	252	271	0.63	252	275	0.74

TABLE IV

Arc Sine Function Using Different Percent of Failure Formula

	ABB (Table IIIc)			ABB Data Using Eqn A(3) /11/
Test Conditions	P 0	P 0.5	r	P 0
N6,R=-1	410	450	0.95	410
N6,R=0	316	350	0.99	321
N9,R=-1	276	310	0.98	274
N9,R=0	248	280	1.00	247

4.5 *Haigh Diagram*

To determine the mean stress effect, the Haigh diagram together with the Goodman equation/12/ is often used. The Goodman equation uses the fatigue strength at R=-1 where the mean stress is zero, and the ultimate tensile strength of the material.

$$\sigma_a / Se + \sigma_m / Su = 1 \qquad (2)$$

where σ_a is the cyclic stress amplitude
σ_m is the mean stress
Se is the fatigue strength at R=-1
Su is the ultimate tensile strength

By using the experimental Se values and assuming Su is 810 MPa (which is the measured axial tensile strength at the bore of the rotor at 100 C/11/), the Haigh diagram for the '0' percent failure (Arc Sine) and the '50' percent failures (Normal Distribution) were drawn. In Figures 8 and 9, the highest 50% fatigue strengths from Table III were used, the 0% fatigue strengths were taken from ABB's estimates (Table IV). The experimental values for R=0 were above the straight line produced by Equation (2).

The limited results indicate that any combination of stress amplitude and the mean stress falling within the triangular envelop will have a safe fatigue life similar to that obtained experimentally for the fatigue strength at R=-1.

5.0 *DISCUSSION*

5.1 *Current Understanding of the Fatigue Limit*

Instead of the zero probability of failure, many of the S-N curves reported in the open literature only provide the fatigue strength at 50% probability of failure. The definition of the fatigue limit in reference 8 is : The horizontal portion of an S-N curve represents the maximum stress that the metal can withstand for an infinitely large number of cycles with 50% probability of failure and is known as the fatigue endurance limit.

For engineering application, a designer normally applies the appropriate safety factor to the fatigue endurance limit and the choice of safety factors depends on the industry. With sufficient test data the B-10 level which represent a 10% probability of failure can be used.

The Normal Distribution has been used in many applications to characterize the failure probability. To confirm that a particular distribution represents the true behaviour, a test sample size of up to 100 is required. It is very difficult to project from limited data to very low probability of failure; different mechanisms of crack initiation may or may not result in the same type of strength distribution.

Recent Japanese work/9/ had successfully applied the Normal Distribution to the data gathered from research over the past 20 years. Most of the data were within the 10% to 95% probability of failure values. All of the fatigue strengths with no failures were found to be below the 10% probability of failure values.

To summarize, our current understanding on the statistics of fatigue data lead towards the use of the Normal Distribution for components exposed to constant amplitude fatigue loading. There is more confidence in predicting the 50%

probability of failure fatigue strength from limited experimental data comp red with a "lower bound" (less than 10% probability of failure) fatigue strength. However, the "lower bound" value can be used as a reference point for selecting the safety factor.

5.2 *Comparison Between the Normal Distribution and the Arc Sine Method*

Although different distributions were assumed, relatively good correlation coefficients (as shown in Table III) were obtained for all the test conditions. For each type of distribution, the least-squares method revealed a straight line correlation between the fatigue strength and the modified probability of failure parameter.

The variation of the 50% probability of failure strength with the type of distribution and the formulae in Appendix III was not significant. The range of values is 8 and 4 MPa for the OH and ABB data respectively.

The difference in the fatigue strength between the normal and the arc sine distribution became significant at low probability of failure. The differences between the '0' and the '0.01' probability of failure strengths are of the order of up to 34 MPa. For the same strength value, we obtained different probability of failure depending on the type of distribution. However, for each type of distribution, using different percent of failure formula did not result in significantly different values for the fatigue strength (14 MPa difference). In general, predictions from a data base centred around the high stress region are always affected by data scatter and errors from incorrect assumptions about the probability distribution.

The fatigue strengths for 0.01 probability of failure from Normal Distribution are generally lower than the zero probability of failure fatigue strengths from the Arc Sine function. As shown in Fig. 5 for N6, R=-1, the zero probability of failure fatigue strength from the Arc Sine function is above an OH failure point; the Normal Distribution calculation showed a lower value. The two distribution are therefore not providing consistent predictions of lower-bound fatigue strengths.

It is possible that the strength distribution flattens out below the 0.01 probability value in the Normal Distribution; at sufficiently low stress, no specimens should fail. The Japanese work/9/ did show a cutoff point, the value was about 10 MPa below the fatigue strength at 0.01 probability. A very large test matrix which is very expensive and time consuming will be required if we want to determine the true distribution for the failure probabilities.

Two sets of OH data had consistently generated low correlation coefficients for all distribution functions. The S-N data plots showed that the N6, R=-1 and N9, R=0 data points are different from ABB's data points. The correlation is poorer for the OH data. However, no such scatter was observed in the other test conditions (N6, R=0 and N9, R=-1) which essentially used the same test procedures, suggesting that this was not an experimental problem. The specimens were also taken from the same general locations. The N6, R=0 and R=-1 samples were from the series A and C, the others were taken from area close to the bore of the rotor.

Due to the small sample size, we cannot determine if the above observations represent data scatter or incorrect assumptions about the distribution. For example, to describe accurately the behaviour at any part of a Normal Distribution, a weighted probit least squares analysis would require about 50 specimens per test condition/10/.

The above demonstrates that there is less scatter at the median value and hence there is more confidence in the prediction of the 50% probability of failure fatigue strength. The recommended values are in the following table:

TEST CONDITIONS AT 100 C	*MEDIAN FATIGUE STRENGTH (MPa)*
N6, R=-1	457
N6, R=0	355
N9, R=-1	320
N9, R=0	278

An appropriate safety factor, normally used in design equation/13/, can then be applied to this fatigue endurance limit during the design process as discussed in section 5.1.

6.0 *SUMMARY*

All three laboratories (OHRD, EMR and ABB) generated very similar fatigue test data. The Normal Distribution, which has been used extensively for many different materials, gave a 0.01 probability of failure for ABB's zero failure fatigue strength based on the Arc Sine equation. However, the median fatigue strengths are close regardless of the distributions used. It is therefore better to use the more exact median value and apply an appropriate safety factor during the design stage.

ACKNOWLEDGEMENT

We thank Dr. A. Hull of Engineering Material Research for carrying out part of the experimental work and the many fruitful discussion with him.

Reviewed by:

B. Mukherjee
Supervising Engineer
Fracture Technology Section

Prepared by:

W.K. Lee
Engineer
Fracture Technology Section

Approved by:

for J. Brown
Manager
Metallurgical Research Department

D.W. Carpenter
Technologist
Fracture Technology Section

REFERENCES

1. M. Clarke, "Metallurgical Investigation of Cracking in Generator Rotor Shaft, Darlington NGS, unit 2", OHRD report no. 91-7-K.

2. Standard Practice for Conducting Constant Amplitude Axial Fatigue Tests of Metallic Materials, ASTM E 466-82.

3. Standard Recommended Practice for Constant-Amplitude Low-Cycle Fatigue Testing, ASTM E 606-80.

4. Weibull, W. "Fatigue Testing and Analysis of results", p198-199, Pergamon Press, 1961.

5. Private communication with Dr. G.Ebi of ABB.

6. Dengel, Dieter. "Die arcsin (P)-Transformation - ein einfaches Verfahren zur grafischen und rechnerischen Auswertung geplanter Wohlerversuche", Z.f. Werkstofftechnik / J. of Materials Technology 6. Jahrgang. Heft 8. Seite 253-288, August 1975.

7. Little, R.E. "Manual on Statistical Planning and Analysis", ASTM, STP 588, p.54.

8. "Atlas of Fatigue Curves", edited by H.E. Boyer, ASM, p.2, 1986.

9. T.Tanaka, T.Sakai and T.Iwaya in "Statistical Research on Fatigue and Fracture", p.125-57, Elsevier Applied Science Publishers, London, UK. 1987.

10. Weibull, W. "Fatigue Testing and Analysis of results", p15-16, Pergamon Press, 1961.

11. J.E. Roynon, "Minutes of Meeting No. 5, Darlington GS-Generator Room Failure, July 16-17, 1990", July 24, 1990.

12. J.A. Bannantine, J.J. Comer and J.L. Handrock, "Fundamentals of Metal Fatigue Analysis", p.6-8, Prentice-Hall, 1990.

13. J.E. Shigley, "Mechanical Engineering Design", 3rd ed., McGraw-Hill, New York, 1977.

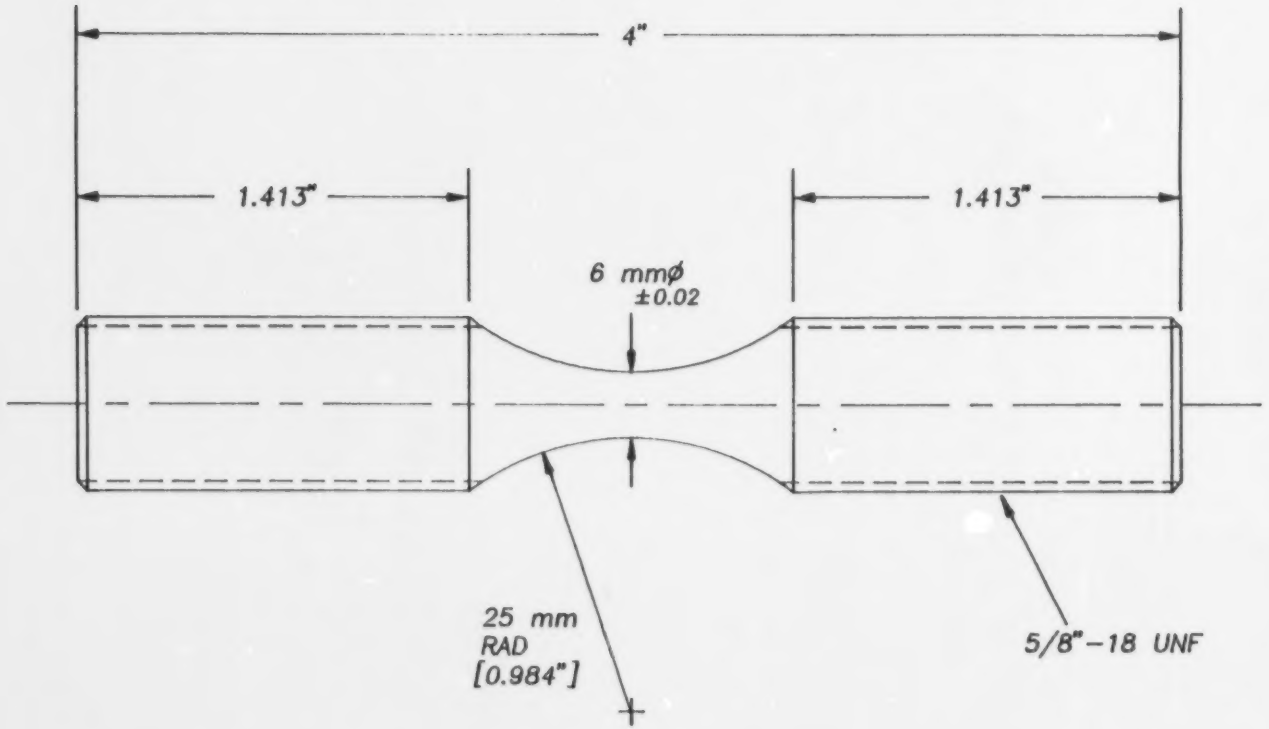

FIGURE 1
HOUR-GLASS FATIGUE SPECIMEN

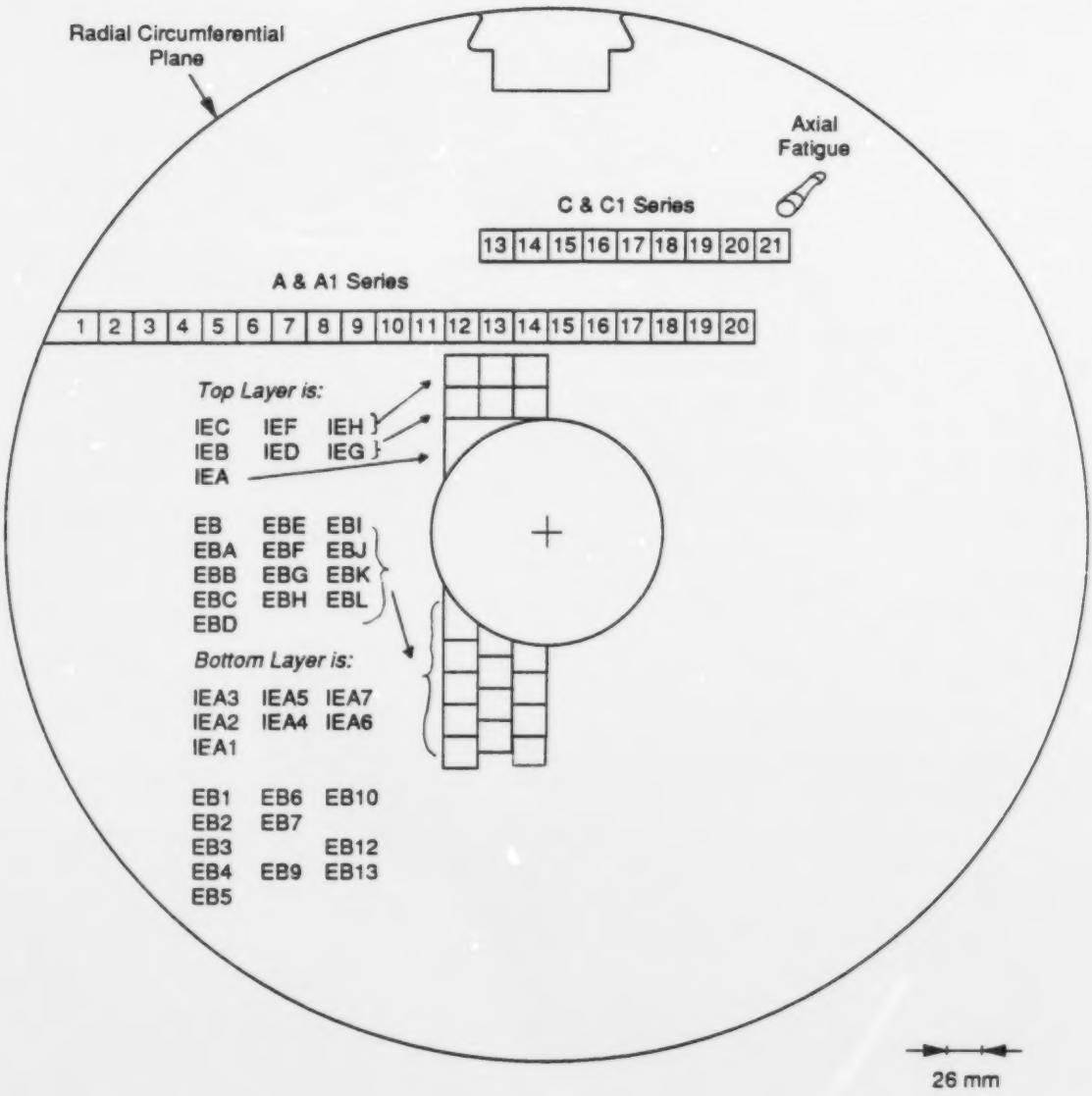

FIG. 2 - LOCATION OF FATIGUE SPECIMENS

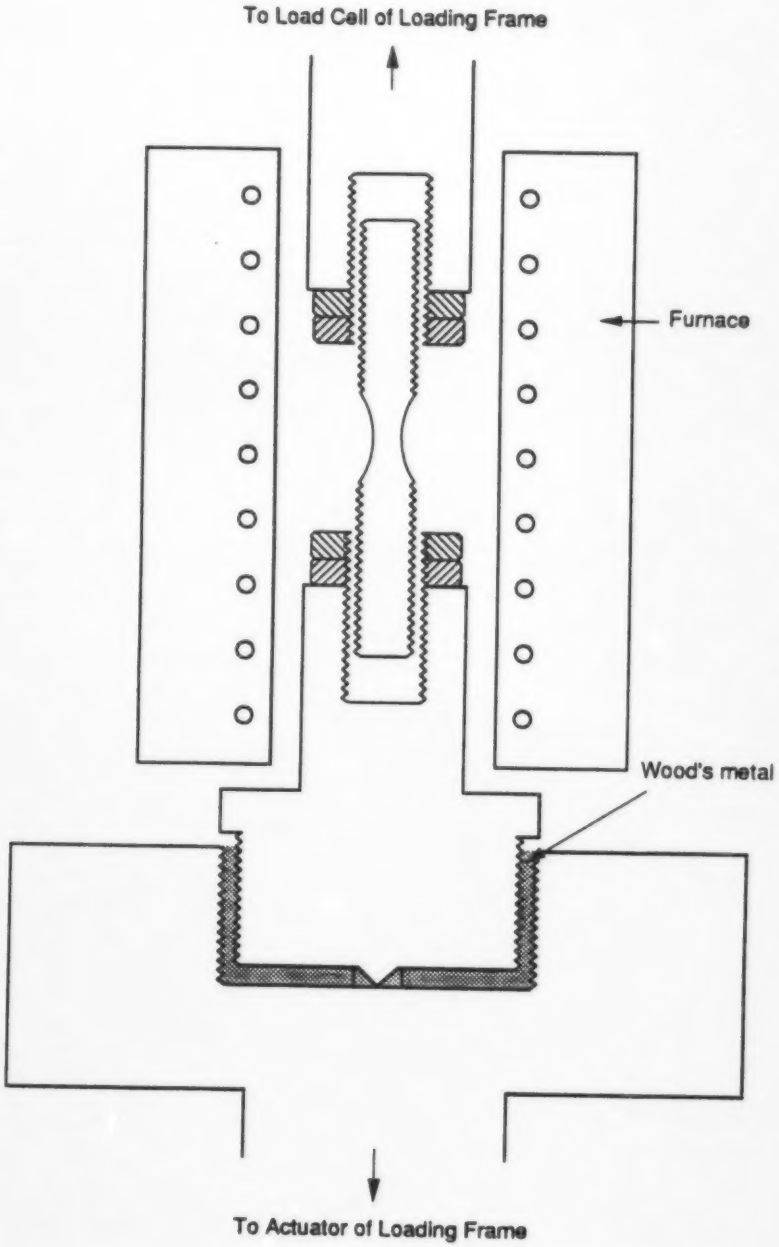

FIG. 3 - SCHEMATIC DIAGRAM FOR LOADING TRAIN

FIG. 4 COMBINED FATIGUE DATA
100 C, R=0

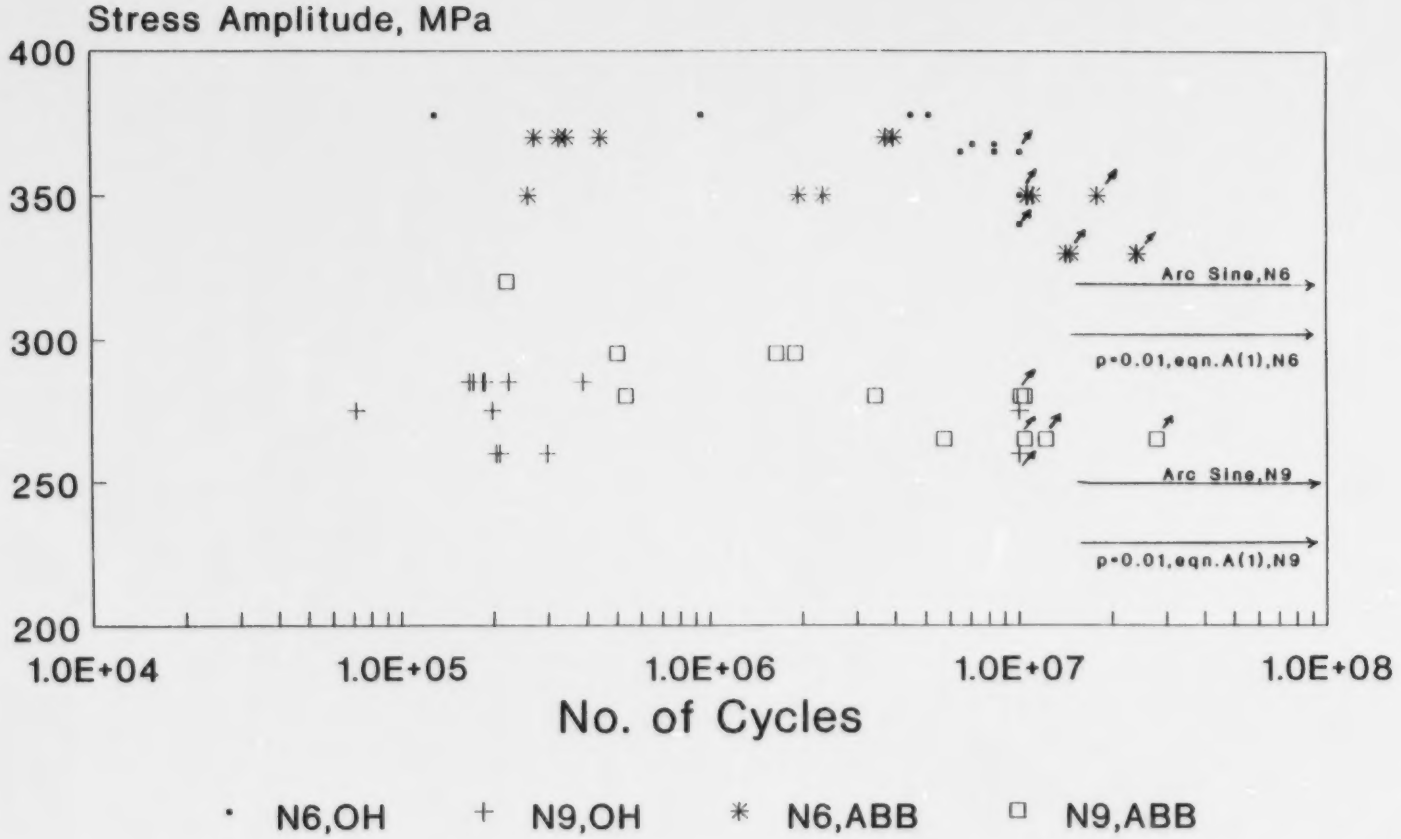

FIG. 5 COMBINED FATIGUE DATA
100 C, R=-1

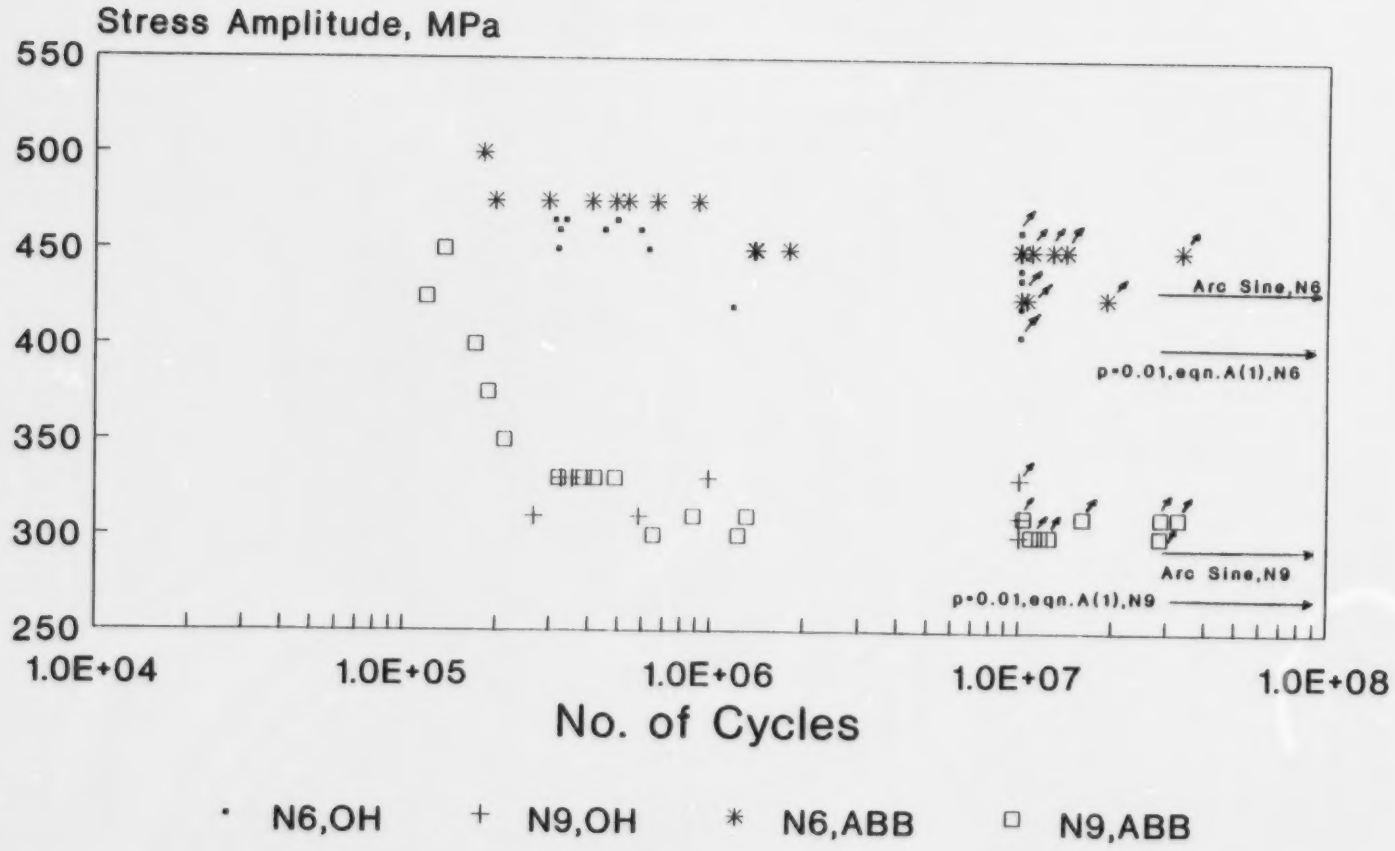

FIG. 6 NORMAL DISTRIBUTION FOR PROBABILITY

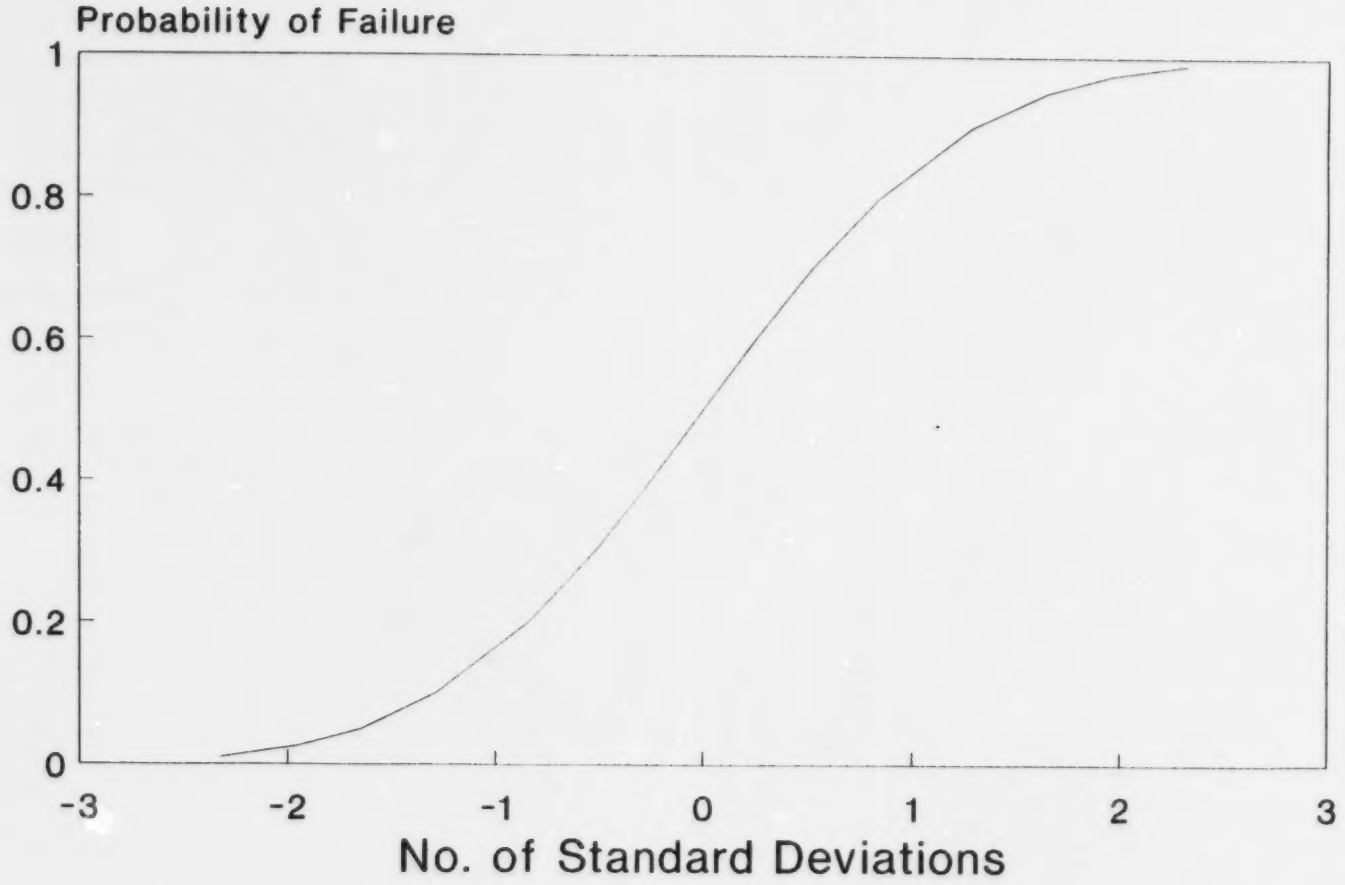

FIG. 7 PROBABILITY OF FAILURE NORMAL DISTRIBUTION, N6,R=0,100C

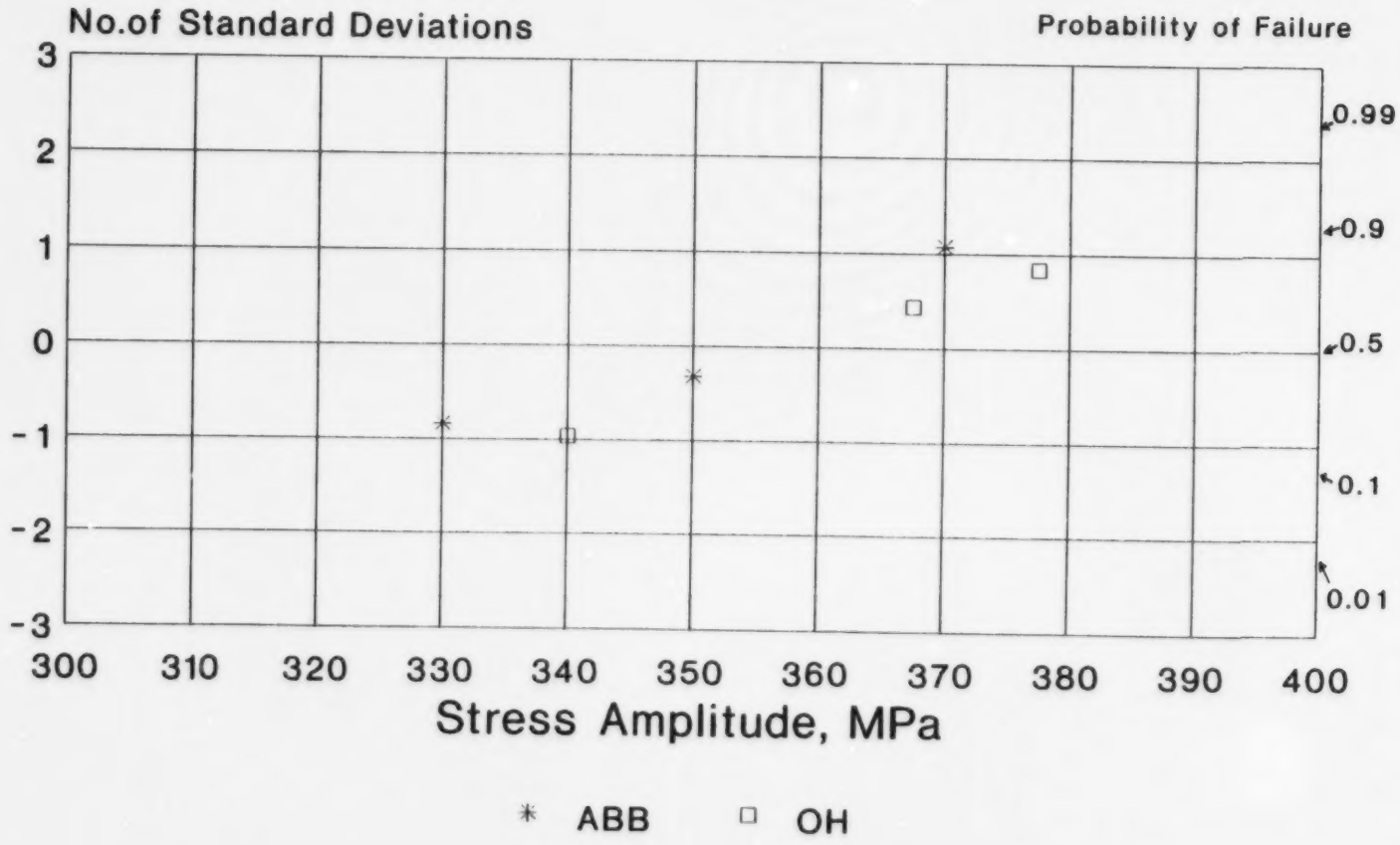

FIG. 8 HAIGH DIAGRAM USING 50 % FAILURE DATA

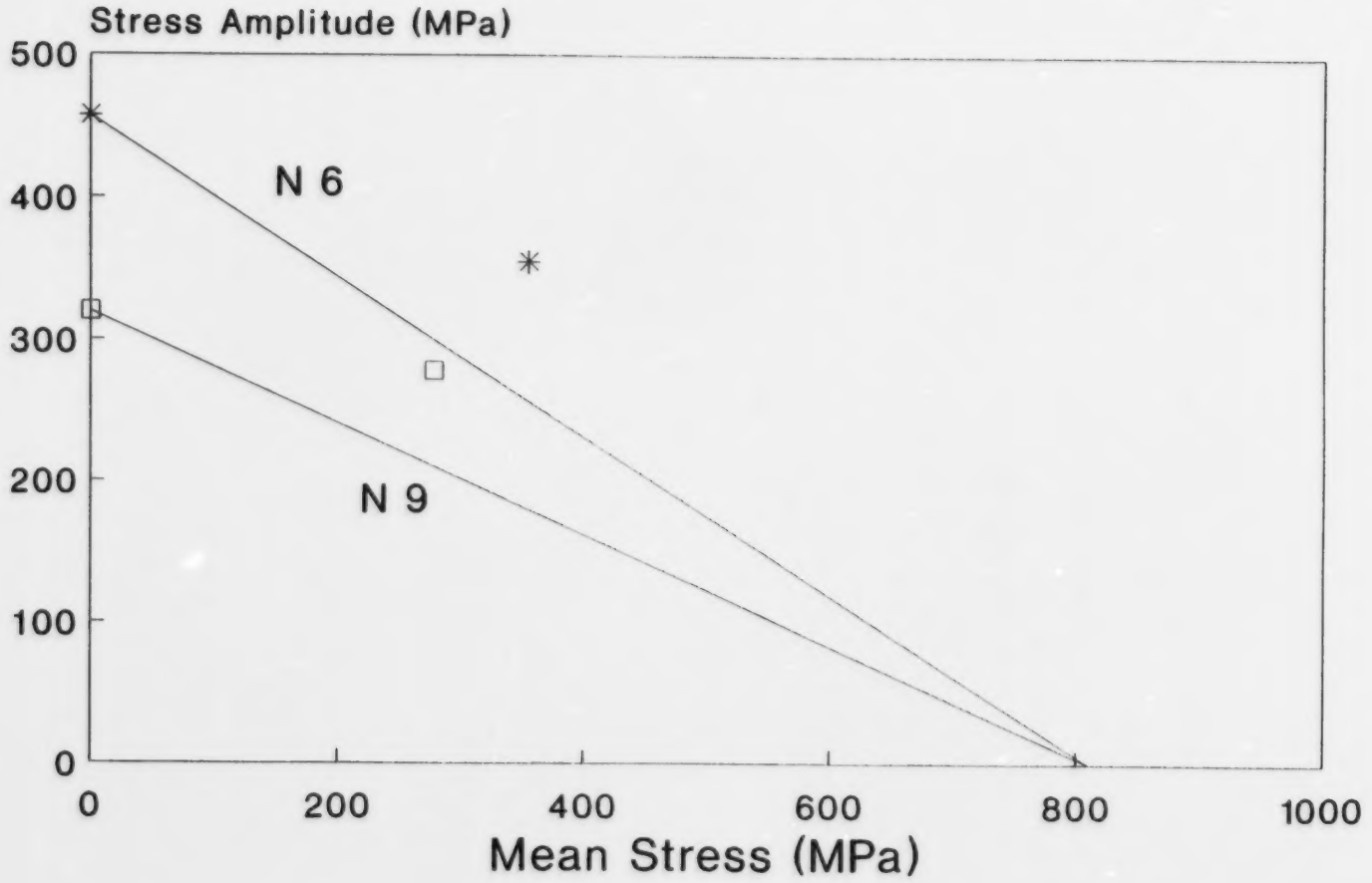

FIG. 9 HAIGH DIAGRAM USING ABB 0 % FAILURE DATA /11/

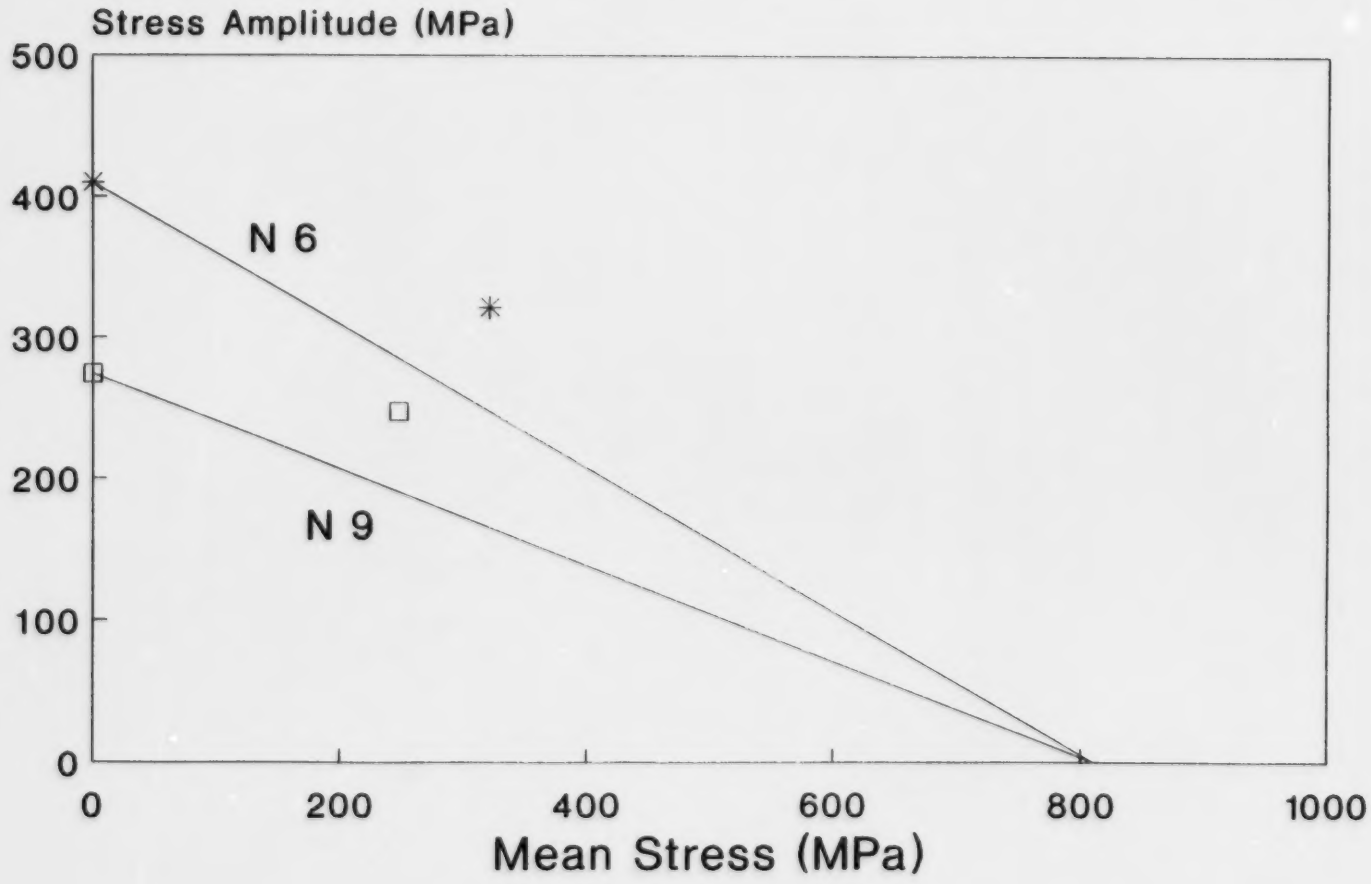

Appendix I
Results of Strain Gauge Measurements to Determine the Axial Alignment

Four strain gauges, 90 degrees apart, were attached to the gauge section of a hour-glass fatigue specimen. The assembly was then placed onto the loading frame, following standard fatigue test procedures. Heat was applied to the Wood's metal holder to melt the low temperature alloy to provide a stress free connection to the loading train. Running water kept it cold during the test. The strains were measured per incremental increase in the load applied to the specimen.

Good alignment was obtained for the two test frames at OHRD and EMR. The deviations were well within the 5% allowed by the ASTM standard E466/2/. Figures I.1 and I.2 show the straight line relation between the applied loads and the strain results. To improve the graphical illustration, offsets from the actual test results (listed in the following tables) were used. Symmetry of axial strain is shown by the lines being parallel.

OHRD results:

10 V = 25 kN, gauge readings in microstrains
Diff. = (Maximum strain - Average strain)/Average strain

APPLIED LOAD (V)	GAUGE 1	GAUGE 2	GAUGE 3	GAUGE 4	MAXIMUM	AVERAGE	DIFF.
0	0	0	0	0			
.5	218	225	226	220	226	222.25	1.7%
1	446	452	456	442	456	449	1.6%
1.5	666	678	676	658	678	669.5	1.3%
2	904	896	904	878	904	895.5	.9%
1.5	680	680	673	674	680	676.75	.5%
1	448	450	443	449	450	447.5	.6%
.5	230	228	221	232	232	227.75	1.9%
0	0	0	0	0			

EMR results:

10 V = 15.6 kN, gauge readings in microstrains
Diff. = (Maximum strain - Average strain)/Average strain

APPLIED LOAD (V)	GAUGE 1	GAUGE 2	GAUGE 3	GAUGE 4	MAXIMUM	AVERAGE	DIFF.
0	0	0	0	0			
.8	140	141	135	138	141	138.5	1.8%
1.6	278	280	272	278	280	277	1.1%
2.3	420	426	410	420	426	419	1.7%
3.1	563	566	553	561	566	560.75	.9%
3.9	710	711	692	706	711	704.75	.9%
4.7	852	851	835	846	852	846	.7%
5.4	995	989	971	986	995	985.25	1.0%
4.7	851	844	833	849	851	844.25	.8%
3.9	712	708	695	707	712	705.5	.9%
3.1	564	564	561	566	566	563.75	.4%
2.3	421	421	413	423	423	419.5	.8%
1.6	279	284	276	280	284	279.75	1.5%
.8	141	143	137	140	143	140.25	2.0%
0	0	0	0	0			

FIG. I-1 OHRD STRAIN RESULTS

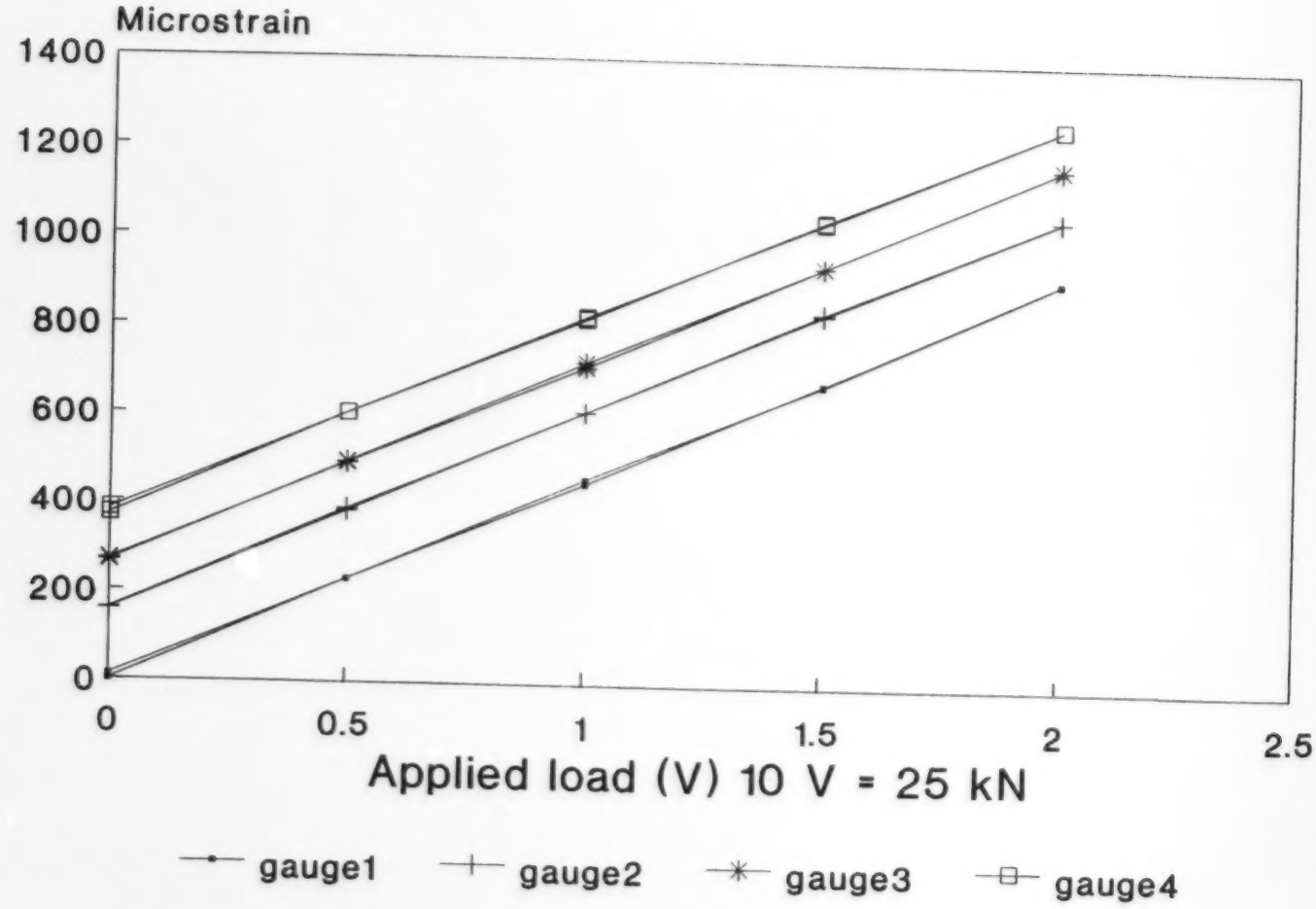

FIG. I-2 EMR STRAIN RESULTS

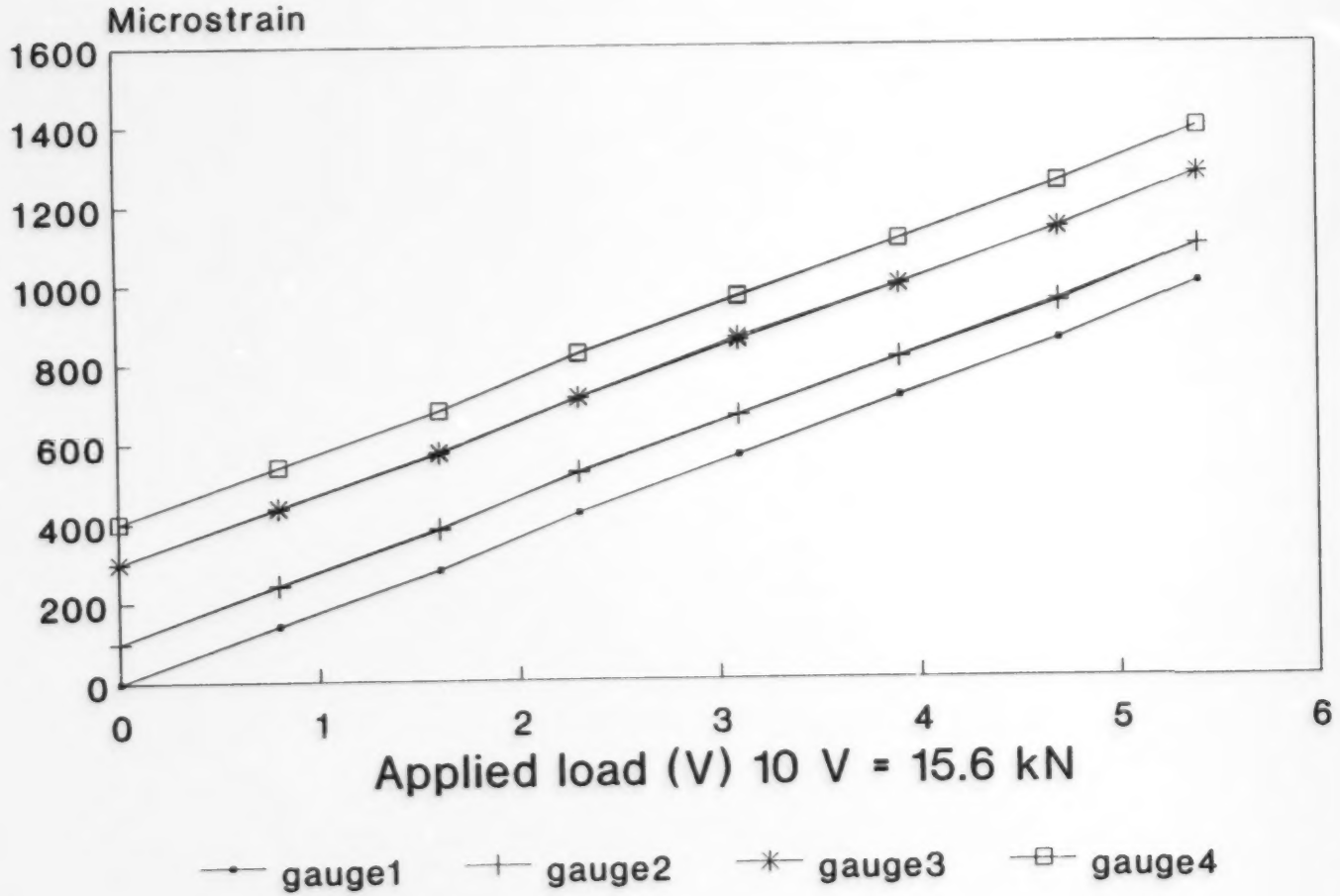

Appendix II

Experimental Results

A thermocouple was attached to the specimen's shoulder; the test frequencies were 15 Hz at OHRD and 30 Hz at EMR.

Table II-I

OHRD and EMR Data at 100 C

Specimen Number	*R Ratio*	*Maximum Stress (MPa)*	*Test Lab.*	*Number Of Cycles*	
----------N6 surface finish----------					
A-7	-1	465	emr	309200	
A10	-1	465	ohrd	492680	
A5	-1	465	ohrd	334490	
A1-5	-1	460	ohrd	320000	
C19	-1	460	ohrd	1.0E+07	
A8	-1	460	ohrd	447690	
C20	-1	460	ohrd	1.0E+07	+347000
A1-2	-1	460	ohrd	585890	
A1-1	-1	460	ohrd	1.0E+07	+133000
C21	-1	460	ohrd	1.0E+07	
A9	-1	450	ohrd	1.0E+07	
A1-6	-1	450	emr	622000	
A1-3	-1	450	emr	1.0E+07	
A4	-1	450	ohrd	315680	
C18	-1	450	ohrd	1.0E+07	
A-8	-1	450	emr	1.0E+07	
A6	-1	450	ohrd	1.0E+07	
C1-20	-1	440	emr	1.0E+07	
C1-19	-1	440	emr	1.0E+07	
C1-15	-1	440	emr	1.0E+07	
C1-14	-1	440	emr	1.0E+07	
A1-20	-1	440	emr	1.0E+07	
C1-17	-1	440	emr	1.0E+07	
C1-16	-1	440	emr	1.0E+07	
C1-18	-1	440	emr	1.0E+07	
A12	-1	435	ohrd	1.0E+07	+135000
A-9	-1	435	emr	1.0E+07	
A1-4	-1	435	emr	1.0E+07	
A-12	-1	420	emr	1170800	
A2	-1	420	emr	1618110	*

*thermocouple weld initiation

Table II-I (Cont'd)

OHRD and EMR Data at 100 C

Specimen Number	*R Ratio*	*Maximum Stress (MPa)*	*Test Lab.*	*Number Of Cycles*	
A-10	-1	420	emr	1.0E+07	
A-11	-1	405	emr	1.0E+07	
A1-16	0	680	emr	1.0E+07	
A1-18	0	680	emr	1.0E+07	
A1-15	0	680	emr	1.0E+07	
A1-17	0	680	emr	1.0E+07	
A1-19	0	680	emr	1.0E+07	
C16	0	700.0	ohrd	1.0E+07	
A17	0	730	ohrd	8348440	
A18	0	730	ohrd	1.0E+07	
A19	0	730	ohrd	1.0E+07	
A20	0	730	ohrd	6467920	
A17	0	735.0	ohrd	8348440	
C17	0	735.0	ohrd	7068730	
A15	0	755.0	ohrd	5114250	
A14	0	755.0	ohrd	128390	
A13	0	755.0	ohrd	4474840	
A16	0	755.0	ohrd	937660	
----------N9 surface finish----------					
IEC	-1	300	emr	1.0E+07	
IEH	-1	300	emr	1.0E+07	
IEA2	-1	300	emr	1.0E+07	
IEA4	-1	300	emr	1.0E+07	
EBK	-1	310	emr	583000	
EBE	-1	310	emr	1.0E+07	
spare	-1	310	emr	266000	near rotor's bore
EB1	-1	310	emr	1.0E+07	
EBF	-1	310	emr	1.0E+07	
1EB	-1	310	emr	1.0E+07	
EBI	-1	310	ohrd	672490	fracture away from gauge
1EA1	-1	310	ohrd	1.0E+07	
1EA3	-1	310	ohrd	1.0E+07	
IEA	-1	330	ohrd	353690	
IEA	-1	330	ohrd	353690	
EBA	-1	330	ohrd	1.0E+07	
EBB	-1	330	ohrd	326970	

Table II-I (Cont'd)

OHRD and EMR Data at 100 C

Specimen Number	*R Ratio*	*Maximum Stress (MPa)*	*Test Lab.*	*Number Of Cycles*
IED	-1	330	ohrd	984190
EB3	-1	330	ohrd	1.0E+07
EBH	-1	330	ohrd	1.0E+07
EB	0	550	emr	71700
IEF	0	550	emr	1.0E+07
IEG	0	550	emr	1.0E+07
EB10	0	550	emr	198200
EB12	0	550	emr	1.0E+07
IEA5	0	550	emr	1.0E+07
EBC	0	570	emr	388500
EBG	0	570	emr	172100
EBJ	0	570	emr	224100
EBL	0	570	emr	184500
EB2	0	570	emr	166900
EB5	0	570	emr	186900
EB6	0	520	emr	1.0E+07
EB7	0	520	emr	1.0E+07
EB9	0	520	emr	208800
EB13	0	520	emr	1.0E+07
EBD	0	520	emr	203900
EB4	0	520	emr	299000

Table II-II

ABB Data at 100 C

Cycle Number	Stress Amplitude (MPa)	R ratio
--------N 6 surface finish		
1.01E+07	425	-1
1.05E+07	425	-1
1.91E+07	425	-1
1.00E+07	450	-1
1.39E+06	450	-1
1.37E+06	450	-1
1.78E+06	450	-1
1.41E+07	450	-1
1.09E+07	450	-1
1.28E+07	450	-1
1.01E+07	450	-1
3.34E+07	450	-1
9.05E+05	475	-1
6.64E+05	475	-1
1.97E+05	475	-1
2.95E+05	475	-1
4.88E+05	475	-1
4.07E+05	475	-1
5.36E+05	475	-1
1.80E+05	500	-1
1.42E+07	330	0
2.39E+07	330	0
1.47E+07	330	0
2.41E+07	330	0
1.94E+06	350	0
1.79E+07	350	0
1.07E+07	350	0
2.59E+05	350	0
1.06E+07	350	0
2.33E+06	350	0
1.11E+07	350	0
3.44E+05	370	0
3.26E+05	370	0
4.44E+05	370	0
3.72E+06	370	0
2.72E+05	370	0
3.94E+06	370	0

Table II-II (Cont'd)

ABB Data at 100 C

Cycle Number	Stress Amplitude (MPa)	R ratio
----------N9 surface finish ----		
1.09E+07	300	-1
1.23E+06	300	-1
1.25E+07	300	-1
6.50E+05	300	-1
2.85E+07	300	-1
1.17E+07	300	-1
1.03E+07	310	-1
1.60E+07	310	-1
3.27E+07	310	-1
2.88E+07	310	-1
8.77E+05	310	-1
1.31E+06	310	-1
1.31E+06	310	-1
4.88E+05	330	-1
4.19E+05	330	-1
3.20E+05	330	-1
3.85E+05	330	-1
3.74E+05	330	-1
2.12E+05	350	-1
1.87E+05	375	-1
1.70E+05	400	-1
1.18E+05	425	-1
1.35E+05	450	-1
1.04E+07	265	0
2.78E+07	265	0
1.22E+07	265	0
5.72E+06	265	0
1.04E+07	265	0
2.78E+07	265	0
5.33E+05	280	0
1.04E+07	280	0
1.01E+07	280	0
3.43E+06	280	0
1.89E+06	295	0
1.64E+06	295	0
5.01E+05	295	0
2.20E+05	320	0

Table II-III

ABB Data at Room Temperature

Cycle Number	Stress Amplitude (MPa)	R ratio
--------N 6 surface finish		
5.12E+05	450	-1
1.80E+07	450	-1
1.34E+07	450	-1
1.12E+07	450	-1
1.21E+07	450	-1
2.37E+07	450	-1
1.58E+07	450	-1
6.32E+07	450	-1
1.01E+07	450	-1
1.01E+07	450	-1
1.18E+07	450	-1
1.22E+06	475	-1
1.27E+07	475	-1
1.01E+07	475	-1
1.12E+07	475	-1
1.01E+07	475	-1
8.62E+05	475	-1
8.03E+05	475	-1
1.18E+06	500	-1
2.49E+05	500	-1
2.11E+05	500	-1
2.90E+05	500	-1

Appendix III

The Percent of Failures

Normal Distribution

There are two formulae widely used to estimate the percent of failures for the population from the number of specimens which have failed for the Normal Distribution/4/:

$$p = i/(n+1) \quad \text{or } 1/(n+1) \text{ if no specimen failed} \qquad A(1)$$

$$p = \{i-(3/8)\}/\{n+(1/4)\} \quad \text{or}$$

$$\{1-(3/8)\}/\{n+(1/4)\} \quad \text{if no specimens have failed} \qquad A(2)$$

where p - estimated percent of failures
i - number of failed specimens
n - number of test specimens

Arc Sine Function

For the Arc Sine distribution, a modified formula was used by ABB/5/ using the same symbols as the above:

$$p = i/n \quad \text{or}$$

$$1/(3n+1) \text{ if no specimens have failed} \qquad A(3)$$

The formula in ref.6 is

$$p = i/n \quad \text{or}$$

$$1/(2n) \text{ if no specimens have failed} \qquad A(4)$$

If all specimens have failed, the percent of failure is equal to

$$1 - \{ \text{ p obtained as if no specimens have failed } \}$$

Tables III-I and III-II show the estimated frequency of failures for the population from test results obtained by the three test laboratories using the above formulae.

Table III-I

Combined OHRD and EMR Test Results

				PERCENT OF FAILURE		
TEST PARAMETERS	STRESS AMPLITUDE	NO. OF TESTS	NO. OF FRACTURES	Eqn A(1)	Eqn A(2)	Eqn A(4)
N6	435	3	0	25	19	17
R=-1	440	8	0	11	8	6
100 C	450	7	2	25	22	29
	460	7	3	38	36	43
	465	3	3	75	81	83
N6	340	5	0	17	12	10
R=0	367.5	2	2	67	72	75
100 C	377.5	4	4	80	85	88
N9	300	4	0	20	15	13
R=-1	310	8	2	22	20	25
100 C	330	7	4	50	50	57
N9	260	6	3	43	42	50
R=0	275	6	2	29	26	33
100 C	285	6	6	86	90	92

Table III-II

ABB Test Results

				PERCENT OF FAILURE			
TEST PARAMETERS	STRESS AMPLITUDE	NO. OF TESTS	NO. OF FRACTURES	Eqn A(1)	Eqn A(2)	Eqn A(3)	Eqn A(4)
N6	450	11	1	8	6	9	9
R=-1	475	7	4	50	50	57	57
RT	500	4	4	80	85	92	75
N6	425	3	0	25	19	10	17
R=-1	450	9	3	30	28	33	33
100 C	475	7	7	88	91	96	93
N6	330	4	0	20	15	8	13
R=0	350	7	3	38	36	43	43
100 C	370	6	6	86	90	95	92
N9	300	6	2	29	26	33	33
R=-1	310	7	3	38	36	43	43
100 C	330	5	5	83	88	94	90
N9	265	6	1	14	10	17	17
R=0	280	4	2	40	38	50	50
100 C	295	3	3	75	81	90	83